White dwarf masses in magnetic cataclysmic variables: multi-temperature fits to *Ginga* data

Mark Cropper,[1] Gavin Ramsay[2,1] and Kinwah Wu[3]

[1]*Mullard Space Science Laboratory, University College London, Holmbury St Mary, Dorking, Surrey RH5 6NT*
[2]*Astronomical Institute, University of Utrecht, Postbus 80000, NL-3508 TA, Utrecht, the Netherlands*
[3]*Research Centre for Theoretical Astrophysics, School of Physics, University of Sydney, NSW 2006, Australia*

ABSTRACT

One method of obtaining the mass of the white dwarf in magnetic cataclysmic variables (mCVs) is through their hard X-ray spectra. However, previous mass estimates using this method give lower limits because the temperature of the plasma in the post-shock region (where the hard X-rays are emitted) is lower than the temperature of the shock itself. In AM Her systems, the additional cooling of the post-shock plasma by cyclotron emission will further lower the derived mass. Here we present estimates of the masses of the white dwarf in 13 mCVs derived using *Ginga* data and a model in which X-rays are emitted from a multi-temperature emission region with the appropriate temperature and density profile. We include in the model reflection from the surface of the white dwarf and a partially ionized absorber. We are able to achieve good fits to the data. We compare the derived masses with previous estimates and the masses for larger samples of isolated white dwarfs and those in CVs.

Key words: accretion, accretion discs – methods: data analysis – stars: fundamental parameters – novae, cataclysmic variables – white dwarfs – X-rays: stars.

1 INTRODUCTION

The mass of the white dwarf in magnetic cataclysmic variable (mCV) systems is one of the principal determinants characterizing the emission from these interacting binaries. The mass is, moreover, a fundamental parameter with implications for every aspect of our understanding of CVs, for example their origins and evolution (Politano 1990; de Kool 1992; Kolb 1993; Wickramasinghe & Wu 1994). The determination of these masses has therefore been a continuing quest in this field.

There are two subclasses of mCVs. In the AM Her systems (or polars), the white dwarf primary has a strong magnetic field (~tens of MG). This magnetic field causes quasi-radial accretion flow in the vicinity of the white dwarf. It also interacts with the magnetic field of the secondary star, forcing the white dwarf into synchronous (or, in some cases, near-synchronous) rotation with the orbit (see Cropper 1990 for a review). As a consequence, the orientation of the incoming accretion stream is approximately constant with respect to the white dwarf magnetic field. When the accretion stream impinges on the white dwarf surface, the kinetic energy of the gas is converted into heat, via an accretion shock, heating up and ionizing the gas. The shock-heated gas thereby radiates X-rays in the keV range by bremsstrahlung emission. Free electrons spiralling in the magnetized ionized gas also emit polarized optical/infrared cyclotron radiation. In the intermediate polar (or DQ Her) systems (IPs) the field is less strong (~few MG), so that the magnetic torques are insufficient to force synchronism (see Patterson 1994 for a

review). The accretion flow is not affected by the white dwarf magnetic field when it is far from the white dwarf. An accretion disc is therefore able to form. Only in the regions close to the white dwarf surface, where the magnetic stress is strong enough, is the matter threaded by the white dwarf magnetic field and accreted quasi-radially. There it forms an arc near the magnetic pole, as for AM Her systems. In a few IPs the field is sufficiently strong that circularly polarized cyclotron emission is detected.

The classical primary methods for measuring the masses of the component stars in a binary system are not generally available in mCVs, and more indirect methods have been used (see Bailey 1995 for a review). One of these methods is to make use of the spectrum of the keV X-rays emitted from the accreting white dwarfs (Rothschild et al. 1981; Kylafis & Lamb 1982; Ishida 1991). The basis of the method is that the temperature of the accretion shock depends on the white dwarf mass and radius, that is $kT_s \simeq 3\mu G M m_p / 8R$ (where k is Boltzmann's constant, T_s is the temperature of the shock, μ is the mean molecular mass, G is the gravitational constant, m_p is the mass of the proton, M is the white dwarf mass, and R is the white dwarf radius). For typical white dwarf parameters, $kT_s \sim 20$ keV. More massive white dwarfs have smaller radii, so the corresponding shock temperatures are higher. A higher shock temperature implies a hotter post-shock region, and hence a harder X-ray spectrum. By fitting model spectra to the observed spectrum the temperature and therefore the white dwarf mass can be deduced. This method was used by Ishida (1991) to measure the white dwarf masses of five AM Her systems and nine IPs from *Ginga* data.

It has been recognized that the observed X-ray spectra are, however, determined by emission contributed from the entire post-shock region, which is a settling column of plasma below the accretion shock, stratified in temperature and density. The temperature in the post-shock region is always lower than the temperature of the accretion shock (Aizu 1973). With the bremsstrahlung emissivity varying only as the square root of the temperature, and as the density squared, most of the X-rays are emitted from the dense, low-temperature region at the bottom. The temperature obtained by spectral fitting therefore reflects mostly the condition of the bottom of the post-shock cooling region. It is obvious that using this temperature will inevitably lead to a severe underestimation of the white dwarf masses.

The situation can be further complicated when additional cooling mechanisms are present. As the white dwarfs in AM Her systems are strongly magnetized, cyclotron cooling is important and it can dominate bremsstrahlung cooling (Lamb & Masters 1979; King & Lasota 1979). The inclusion of cyclotron cooling lowers the average temperature of the emission region, and hence softens the X-ray spectrum. Omission of the cyclotron cooling will lead to further underestimation of the white dwarf masses.

Effects of cyclotron cooling on accretion shocks were first considered in the numerical studies by Langer, Chanmugam & Shaviv (1982). The focus of their studies was, however, the stability properties of the accretion shock rather than the structure of the post-shock region and its radiation. A comprehensive numerical study of the shock structure and its emission was carried out by Woelk & Beuermann (1996). As the effects of angle-dependence of the cyclotron cooling function and the optical depth were treated explicitly, this study yielded accurate results. Although the calculations by Woelk & Beuermann (1996) can determine the structure of the post-shock region accurately, because of the numerical nature of the formulation, it not easy to apply it in a practical situation such as determining the white dwarf masses.

Wu, Chanmugam & Shaviv (1994) considered an analytic approach for the purpose of obtaining reasonably accurate results that are more readily usable. In their formulation, an effective composite function is constructed to mimic the total cooling processes, and a closed-form solution was obtained. This greatly simplifies the computation processes and hence the data fitting. Nevertheless, as the cooling function is an approximation, the shock structure may not be as accurate as those obtained from numerical studies in which the angle-dependent cyclotron cooling is treated explicitly.

Making use of their analytic formulation, Wu, Chanmugam & Shaviv (1995) considered an effective temperature weighted by the contribution from different strata in the post-shock regions and re-adjusted the white dwarf masses given by Ishida (1991). The mean of the white dwarf masses re-adjusted by Wu et al. (1995) is in better agreement with those obtained by other methods. However, this approach neglected the density weighting. Moreover, the data should be fitted with a multi-temperature model at the start, and complicating factors such as the reflection, or partial covering found in AM Her by Beardmore et al. (1995a), should also be included at that time.

Another investigation along this line was carried out by Done, Osborne & Beardmore (1995) for the AM Her system EF Eri. However, the temperature profile used in their model is approximated by a cooling flow model (i.e. the temperature and density structures were not calculated explicitly by considering the bremsstrahlung and cyclotron cooling).

In this investigation we take a step further by treating the cooling process in a more precise manner, using the closed integral solution of Wu et al. (1994) to determine the temperature and density structures of the post-shock region. We calculate the integrated emission from it and the resulting spectra are used to refit the *Ginga* spectra of five AM Her systems and eight IPs to determine their white dwarf masses.

2 THE MODEL

Before proceeding further, it is necessary to review the structure of the accretion region and the way this can be modelled appropriately. The structure of the accretion region in AM Her systems was first investigated in detail by Masters (1978) and Lamb & Masters (1979). The infalling gas, threaded by the magnetic field, accretes quasi-radially, forming a strong shock. The hot gas in the post-shock region emits X-rays as it cools by bremsstrahlung emission, and in the optical and near-infrared by cyclotron radiation. Approximately half of the X-rays are intercepted by the surface of the white dwarf, and are reprocessed as soft X-rays.

While this paradigm has remained essentially valid, there have been significant changes in our perception of the mechanism of X-ray emission since it was proposed. First of all there is strong evidence of an excess in the observed soft X-rays in comparison to the hard X-rays (Ramsay et al. 1994). This is difficult to reconcile with the 'standard model' of Lamb & Masters (1979), in which the soft X-rays are due to reprocessing. To explain the soft X-ray excess, Kuijpers & Pringle (1982) proposed an alternative scenario in which the accretion is not smooth and homogeneous: high-density 'blobs', which are formed in the upstream of the accretion column due to instabilities, are embedded in the smoother flow of lower density gas. Many mini-accretion regions will be formed when the dense blobs impact on the white dwarf. The blobs can penetrate deeply into the white dwarf atmosphere, and are partly or wholly buried (Frank, King & Lasota 1988). While the hard X-ray emission may arise from the more finely divided flow, as before, and from the unburied parts of the mini-accretion columns (Ramsay, Cropper & Mason 1995), the soft X-rays are emitted from the part of the white dwarf atmosphere thermalized by the hard X-rays emitted from the deeply buried accretion blobs.

Moreover, the asymmetries in the optical/infrared light curves, including those from the polarization data, indicate that the shock-heated emission region is extended (Beuermann, Stella & Patterson 1987; Cropper 1987), probably into arc shapes (see e.g. Wickramasinghe 1988), with large variations in the specific accretion rate across it. As the dominant cooling process depends on the local accretion rate, large variations in the local accretion rates may lead to breaking down of the accretion shock at the low accretion rate regions (the non-hydrodynamic regime of Masters 1978). Consequently, some regions in the accretion arc may not be shock-heated and will be inefficient in emitting hard X-rays.

Other scenarios proposed in the last decade include a photosphere depressed below the local mean scale due to a large ram pressure for very high local accretion rates (Beuermann 1988; Stockman 1988), splashes from the accreting material and 'spaghetti' accretion, where only certain field lines channel accreting material (Andronov 1987).

Although the basic physical processes in the case of IPs are similar, the arc is considered to be even more extended, into an 'accretion curtain' (Rosen, Mason & Córdova 1988), and the specific accretion rate may be lower than in AM Her systems.
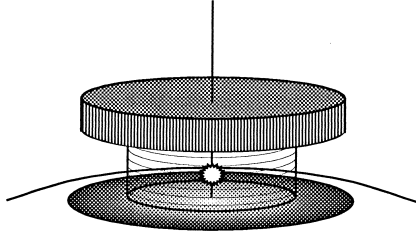
Figure 1. The assumed structure of the accretion region on the surface of the white dwarf including an ionized absorber above the column and a reflection component from the white dwarf surface. For the purposes of the ionization flux for the absorber, the emission from the structured accretion column is assumed to be concentrated halfway up the post-shock region (as denoted by the white spot).

Against this background, it is clear that the physical structure of the accretion region used in the modelling will have significant effects on the predicted spectra. This structure will probably be different from system to system, depending on how the accreting material threads on to the magnetic field, and different from epoch to epoch within any one system, depending on the accretion rate. The opportunities for sophisticated modelling are therefore boundless, but for this investigation, we have opted for a simple model (Fig. 1) in which the bremsstrahlung X-ray flux is emitted from a single, cylindrical structure, with radius R_c and constant specific accretion rate $\dot{m}(r)$ (where r is the distance from the central axis), as described in Wu (1994). Above this structure we have included a warm absorber. To calculate the photoionization of the absorber we use the emission generated from the structured accretion column, and we approximate this by a point at the mid-height of the column. We have also included the effects of the X-ray albedo causing reflection from the surface of the white dwarf. We have not included a soft X-ray component because it will not be visible in the *Ginga* bandpass, but a fluorescent Fe line and absorption by cold inter-stellar material have been included as usual in these systems by the use of standard routines in XSPEC (Arnaud 1996). The multi-temperature emission model, warm absorber and reflection component are particular to this investigation, and so are discussed in more detail in the sections below.

2.1 Multi-temperature emission

To calculate the temperature and density structure of the X-ray emission region, we use the formulation given in Wu (1994) and Wu et al. (1994).[1] Equation (5) in Wu et al. (1994) is the differential equation determining the velocity profile of the accretion flow. The flow velocity as a function of the distance above the white dwarf surface can be obtained by inverting the result from direct integration of the differential equation. The pressure and density profiles can then be calculated as prescribed at the beginning of section 3 of Wu et al. (1994), and with the equation of state of an ideal gas, the temperature profile can also be determined.

---

[1]Wu (1994) is more informative on the details of the derivation. Note that there are several typing errors in the paper that should be noted: (1) there should be a positive sign instead of the negative sign in front of the last term equation (A1); (2) the factor $1/(\gamma - 1)$ should apply to all terms in the right-hand side of equation (A3); (3) in equation (A5), there is a negative sign for the term Λ; (4) the sign for second term at the left-hand side of equation (A7) should be negative, not positive; and (5) in equation (B5) the term before the square root should be $AC^2/u^2\tau^2$. In addition, the bremsstrahlung spectra in fig. 3 are incorrectly normalized.

The flow profile in the formulation given in Wu et al. (1994) is normalized, and hence it does not depend explicitly on the white dwarf mass. However, to determine the ratio of the cyclotron to the bremsstrahlung cooling, one requires information about the magnetic field B, the local specific accretion rate (the total accretion rate can be determined by multiplying this rate – assumed constant with column radius for this investigation – by the area of the column), as well as the free-fall velocity at the white dwarf surface (which is determined only by the mass and the radius of the white dwarf). Moreover, the normalization for the velocity profile also depends on the free-fall velocity and the specific accretion rate. In our calculations, the Nauenberg (1972) approximation for the white dwarf mass–radius relationship is used, which approximates the Hamada–Salpeter (1961) mass–radius relation for carbon white dwarfs to within 4 per cent over the range 0.3 to 1.2 M$_\odot$.

The integration scheme is a simple summation. The number of velocity subdivisions (and hence the number of strata) is set as a parameter in the fitting. To permit more rapid calculations, coarser grids (typically 10) are used for the initial fitting and a finer mesh (up to 250) for refining the fits. The effect in moving between these extremes is a reduction factor of < 5 per cent at all energies for the finest grid as a result of adopting the high edge value of each mesh point rather than the central value: the spectral slope and therefore the mass determination are not significantly affected. The temperature and density for each mesh point are then calculated, together with the volume for this stratum, given by the derived height multiplied by the area of the column. The velocity and temperature structure from our calculations were compared to Wu et al. (1994) figs 1 and 2(a) and confirmed to be in agreement.

In order to fit this multi-temperature model to the X-ray observations we have integrated it into the XSPEC X-ray spectral fitting package (Arnaud 1996). The grid of pressure, temperature and emitting volume, together with metallicity, permits the emission from any optically thin model to be calculated by integration of the emission from each of the vertical strata. A multi-temperature bremsstrahlung spectrum can be calculated, as in Wu (1994) or Wu et al. (1995), but, for this investigation, we have used the MEKAL optically thin plasma code within XSPEC to calculate both continuum and line emission from each stratum. This code is an updated version of the MEKA code (Mewe, Gronenschild & van den Oord 1985), with improvements described in Mewe, Kaastra & Liedahl (1995).

MEKAL is one of the four most widely used optically thin plasma codes that are available (see Brickhouse et al. 1995), and we are aware that there are non-negligible differences between the predicted spectra of these codes. Our choice of MEKAL is because of its explicit treatment of the density as one of the input parameters, whereas, for example, in the Raymond–Smith models, which are also available within XSPEC, density is not treated as an input parameter. Nevertheless, our routines are written in a format in which any of those optically thin plasma codes can be used with only minor modification.

In Fig. 2 we compare the spectrum from a single-temperature plasma at the shock temperature T_s and immediate post-shock density (case a), that from a stratified shock with only bremsstrahlung cooling (case b), and that from a stratified shock with both bremsstrahlung and cyclotron cooling (case c). In each case the mass of the white dwarf is 0.6 M$_\odot$, the local accretion rate is $1\,\mathrm{g\,cm^{-2}\,s^{-1}}$, the radius of the column is 10^8 cm and the metallicity is solar. In the last case the magnetic field $B = 40\,\mathrm{MG}$. The distance assumed is 100 pc. The salient points from this comparison are as
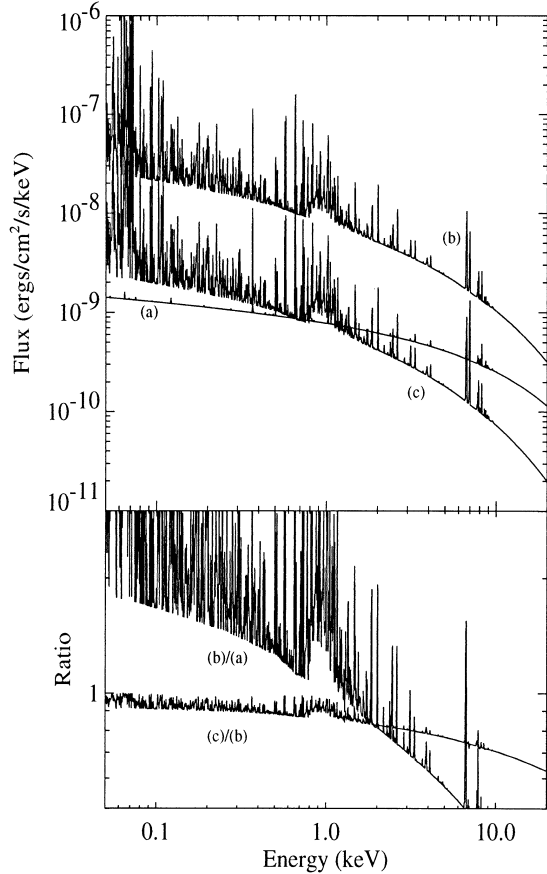
Figure 2. Upper plot: the spectrum from a single-temperature plasma [at the shock temperature T_s (case a)], that from a stratified shock with only bremsstrahlung cooling [displaced vertically by a factor of 10 for clarity (case b)], and that from a stratified shock with both bremsstrahlung and cyclotron cooling (case c). Lower plot: ratios of case (b) to (a), and of case (c) to (b). See text for details.

follows:

(i) the spectrum progressively steepens from case (a) to case (c): this can be understood from the presence of plasma in the column at temperatures cooler than T_s;

(ii) the overall flux decreases from case (a) to case (c) for the same reason;

(iii) the line spectrum becomes progressively richer from case (a) to case (c), partly because of the stronger line emission at lower temperatures, and also because the range of temperatures favours the emission of a broad range of lines, each at its optimal temperature.

2.2 The warm absorber

It is clear from the intensity of the X-ray flux in the post-shock region that the pre-shock flow will be at least partially ionized. This flow will partially absorb the emission from the post-shock region, with the characteristics of the absorption dependent on the ionization state of the infalling material, itself set by the intensity and spectral characteristics of the ionizing flux from the post-shock region below it.

We have therefore modified the ionized absorber model available in XSPEC, ABSORI, to take this absorption into account.

ABSORI (Zdziarski & Magdziarz 1996) is a realization of the model by Done et al. (1992: appendix B) which assumes a power-law photoionizing spectrum. Here we have replaced the power law to permit any form of ionizing spectrum, for example the spectrum calculated for the XSPEC model fits. Our model suffers from the same limitations as ABSORI: there is a single zone of absorption only (so that the radiation transfer is not treated correctly), scattering effects and bound–bound and free–free transitions are not considered. In addition, the recombination coefficients are used outside the density range strictly permitted by the Aldrovani & Pequignot (1973) formulation. Nevertheless, the model should be adequate as a first approximation and is sufficiently rapidly computable to be used in an optimization scheme as in XSPEC.

The warm absorber model requires the ionization of the pre-shock gas to be dominated by photoionization. Although it is unclear whether other mechanisms are important, evidence of photoionization being the dominant mechanism is shown in the eclipse mapping study of the accretion flow in the AM Her system HU Aqr (Hakala 1995). As in ABSORI, ions of 10 elements (H, He, C, N, O, Ne, Mg, Si, S and Fe) are considered, and the photoionizing spectrum is assumed to run from 5 eV to 50 keV. The photoionization cross-sections are falling as ν^{-3} above 10 keV, so that truncating this spectrum at 50 keV is justified.

The upstream flow is cold in the Masters (1978) formulation, but the photoionization will lead to a temperature gradient within the flow. In addition, there is a warm pre-shock region in the flow ahead of the shock, where the electrons and, to a lesser extent, the ions are heated by the fastest particles of the velocity distribution in the material at the shock front (see for example Imamura et al. 1987). We have therefore permitted temperatures for the ionizing absorber in the range 10^3 to 10^6 K, the range over which the approximations for the recombination coefficients are valid.

The effect of the ionized absorber is shown in Fig. 3. Here the absorption is shown for a hydrogen column density of 10^{22} cm^{-2}, temperature of 10^5 K and solar abundances. The assumed electron number density is 10^{16} cm^{-3} and the ionizing flux is a 10-keV bremsstrahlung spectrum of luminosity 10^{32} erg s^{-1} – typical values for AM Her systems. We assume that the ionizing source can be approximated by a point source at half the height of the accretion column and therefore that the absorber is effectively this distance from it (see Fig. 1) – we have used a distance of 5×10^7 cm, yielding an ionization coefficient (Buff & MacCray 1974; Hatchett, Buff & McCray 1976; Lightman & White 1988; Done et al. 1992) of $\xi = 4.0$. For comparison, we have included the absorption from a cold absorber using the cross-sections of Morrison & McCammon (1983).

2.3 The reflection component

Beardmore et al. (1995a) found it necessary to include a reflection component in their model fits to *Ginga* AM Her spectra, both in order to fit the continuum with a single temperature and in order to account for the equivalent width of the observed Fe line. The reflection was from the white dwarf surface. In our case we have a multi-temperature prescription for the continuum, but the equivalent width and energy of the Fe line in those AM Her and other *Ginga* data (below) still suggest that the line flux is augmented by fluorescence, indicating that we may still need to include a reflection component. Moreover, self-consistent numerical calculations of the reflected hard X-ray spectrum have now recently become available (van Teeseling, Kaastra & Heise 1996) which include the temperature structure of the irradiated atmosphere. These
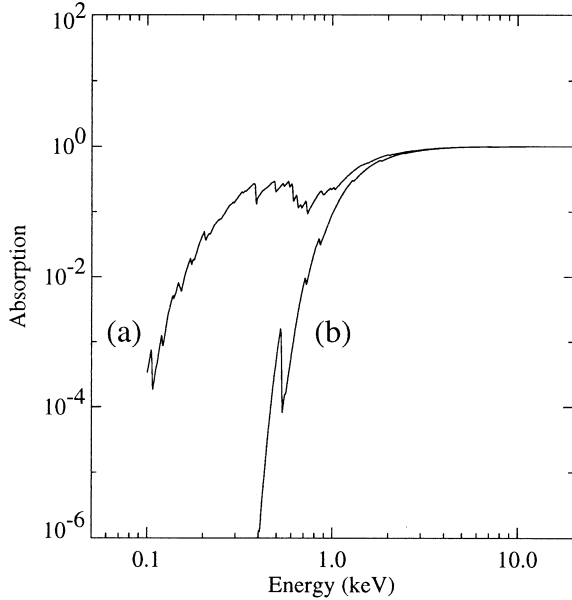
Figure 3. The absorption from a partially ionized absorber for a bremsstrahlung photoionization spectrum (a) and compared to a cold absorber (b). See text for the input parameters.

Table 1. The log of *Ginga* observations of AM Her (upper) and IP stars (lower) used in this study. (1) Beardmore et al. 1995a, (2) Done et al. 1995, (3) Ishida et al. 1991, (4) Ishida 1991, (5) Beardmore et al. 1995b, (6) Rosen et al. 1991, (7) Norton et al. 1992a, (8) Norton et al. 1992b, (9) Ishida et al. 1992, (10) Mason et al. 1992.

Source	Date of Observations	Mean Ct s^{-1}	Reference
AM Her	1989 Sept 17–21	40	(1)
EF Eri	1988 Nov 30–Dec 3	30	(2)
BY Cam	1988 Feb 7–11	20	(3)
V834 Cen	1990 Feb 10–13	4	(4)
QQ Vul	1991 April 9–10	1.5	(5)
EX Hya	1988 Jun 16–17	70	(6)
AO Psc	1990 Jul 10–11	23	(4)
FO Aqr	1988 Oct 29–31	15	(7)
TV Col	1987 Sept 21	22	(4)
BG CMi	1988 Nov 28–29	12	(8)
TX Col	1990 Jan 22–25	10	
GK Per	1987 Sept 22–24	9	(9)
PQ Gem	1991 May 4	9	(10)
AE Aqr	1988 June 1–3	2	

calculations indicate that the contribution from this component, although relatively small (∼10 per cent at 20 keV and less at lower energies), is nevertheless significant.

A full treatment of the reflection component would integrate the illumination from each stratum in the post-shock column of gas at each annulus about its central axis, preferably taking into account the curvature of the white dwarf surface. This would fix the temperature structure in the surface as a function of radius from the column, which, with the incident flux, could be used to calculate the albedo as a function of viewing angle and energy. This is beyond the scope of this paper. We have therefore proceeded by using the analytic approximation supplied by van Teeseling et al. (1996) (their equation 11). This approximation is applicable only to angle-averaged illumination. On the other hand, the angular dependence in their fig. 7 is integrated over energy. However, given that the shape of the energy dependence at two extreme viewing angles 14°.9 and 88°.1 (the upper and lower lines in their fig. 6) is almost unchanged, we have simply used fig. 7 of van Teeseling et al. (1996) to scale the angle-averaged albedo calculated from their equation (11). We checked that the results for 14°.9 and 88°.1 agreed with those shown in their fig. 6. We assume that 2π sr of the flux from the accretion column is intercepted by the white dwarf surface and incorporate a cosine dependence to take account of the projected area reduction at larger viewing angles. We calculate or estimate the viewing angle to the region (see below) and we add the reflected component to the direct component from the accretion column. Both are assumed to be absorbed by the partially ionized absorber.

Note that the viewing angle (referred to as the inclination) in van Teeseling et al. (1996) is the angle to the reflecting site, and it is assumed that this site is illuminated uniformly (van Teeseling, private communication). In these systems the angular dependence of the illuminating (as opposed to the reflected) rays may also be important, and may modify the temperature structure of the atmosphere, and the albedo.

We have chosen for this investigation not to use the predictions of van Teeseling et al. (1996) for the Fe fluorescence line fits, but have

allowed the normalization of the line to be fitted as a free component.

3 MODEL FITS TO *GINGA* DATA

3.1 Observations

We now use the models discussed in Section 2 to fit spectra extracted from data obtained using *Ginga* (1.7–37.0 keV: Turner et al. 1989) to obtain estimates of the mass of the white dwarf in a number of mCVs. Data were extracted for eight AM Her systems and nine IPs from the UK *Ginga* public data archive in Leicester. Of these, two AM Her systems (QS Tel and ST LMi) were too faint to be of use in these fits, and in another (BL Hyi) the background subtraction is problematic. In the case of GK Per (an IP), unsatisfactory fits were obtained (see below). The resulting data set consists of five AM Her systems and eight IPs. Many of the data have been discussed elsewhere (e.g. Ishida 1991): for convenience we show in Table 1 the dates of observation, the mean intensity and references for previous work.

The source data were background subtracted using data of nearby 'blank' areas of sky taken before or after the observation. Data with enhanced background were also removed before analysis. Spectra were extracted in 48 pulse-height channels and fitted using XSPEC with the modified warm absorber, the multi-temperature emission model with and without a reflected component from the white dwarf surface, and an additional iron line at about 6.4 keV when the data required it. In the fitting process, data above ∼20 keV were not used as the signal-to-noise ratio was generally low. As it was likely that spectral variations would be present in the data, either from absorption effects or from two accretion poles contributing to the X-ray flux, we extracted data from different spin phases (typically the brightest phase).

We made various assumptions regarding the warm absorber model: we fixed the distance to the CV at the distance quoted in Warner (1995), or at 100 pc when the distance was not known. The temperature of the ionized absorber was fixed at 10^6 K. Further, we assumed the iron abundance in the ionized absorber was equal to

Table 2. The best-fitting parameters to the *Ginga* data using the modified warm absorber and the multi-temperature bremsstrahlung model. The following parameters are shown: the hydrogen column density of the warm absorber (N_H), the iron abundance, the ratio of cyclotron to bremsstrahlung cooling at the shock (ϵ_0), the specific mass accretion rate ($\dot{m}$), the radius of the accretion column (r_c), the mass of the white dwarf (M_{wd}) both including a contribution from reflection of the surface of the white dwarf and without one. The range in the white dwarf mass is at the 90 per cent confidence range. For AM Her and FO Aqr we simultaneously fitted more than one spin-resolved data set with the column density of the warm absorber being allowed to vary.

Source	N_H 10^{22} cm^{-2}	Iron rel solar	ϵ_0	$\dot{m}$ $g\,s^{-1}$ cm^{-2}	r_c cm $\times 10^9$	M_{wd} ($M_\odot$) no reflection	χ^2 (dof)	M_{wd} ($M_\odot$) with reflection	χ^2 (dof)
AM Her	17–22	0.2	20.0	0.12	0.042	1.25 (1.15–1.35)	0.93 (101)	1.22 (1.15–1.30)	0.86 (100)
EF Eri	0.7	0.4	0.3	1.4	0.016	0.92 (0.85–1.00)	1.00 (21)	0.88 (0.82–0.94)	1.00 (21)
BY Cam	25	0.3	10	0.7	0.017	1.09 (1.02–1.30)	1.48 (23)	1.06 (1.00–1.25)	1.43 (22)
V834 Cen	29	0.7	0.4	1.0	0.016	0.52 (0.25–1.00)	0.88 (22)	0.51 (0.25–1.00)	0.88 (21)
QQ Vul	8.8	1.0 (fix)	20.0	1.0	0.016	1.13 (0.95–1.30)	1.27 (23)	1.12 (0.95–1.30)	1.29 (22)
EX Hya	0.2	0.7	0.001	0.001	1.0	0.54 (0.42–0.60)	0.62 (25)	0.52 (0.40–0.60)	0.65 (24)
AO Psc	16.0	0.4	0.001	0.9	0.09	0.41 (<0.80)	0.93 (21)	0.39 (<0.80)	0.93 (25)
FO Aqr	15–22	0.2	0.001	0.2	0.06	1.20 (>1.00)	0.82 (48)	1.24 (> 1.0)	0.79 (47)
TV Col	40.0	0.5	0.001	0.006	0.046	1.35 (>1.0)	0.84 (21)	1.15 (>0.95)	0.85 (21)
BG CMi	22.0	0.6	0.001	0.44	0.082	1.30 (1.16–1.39)	0.60 (17)	1.22 (1.05–1.30)	0.62 (17)
TX Col	4.3	0.2	0.001	0.7	0.08	0.56 (0.44–0.64)	1.37 (25)	0.55 (0.44–0.64)	1.34 (25)
PQ Gem	4.0	1.0 (fix)	0.001	0.15	0.03	1.39 (>1.25)	1.09 (16)	1.35 (>1.05)	1.09 (16)
AE Aqr	5.3	1.0 (fix)	0.001	1.0	0.01	0.30 (<1.15)	0.76 (19)	0.31 (<1.15)	0.76 (19)

that in the accretion flow. Thus we had eight free parameters: N_H (one component due to the interstellar absorption and one from absorption due to the warm absorber), Z (metal abundance), N_e, h (the distance between the source and the absorber), $\dot{m}$, r_c (the radius of the column) and M_{wd}. A normalizing factor was fixed at $1/d_{pc}^2$. The ratio of cyclotron to bremsstrahlung cooling at the shock (ϵ_0: see Wu et al. 1995) was fixed in such a way that the magnetic field as inferred by inverting equation (10) of Wu et al. (1994) matched that of the magnetic field strength of the system being fitted (we took the magnetic field strengths from Beuermann & Burwitz 1995). Because cyclotron cooling is unimportant for IPs, we simply fixed $\epsilon_0 = 0.001$ for those systems: this gave inferred magnetic field strengths of $B = 1 - 5\,MG$. A further parameter, the viewing angle, was required when we included a reflected component as were three additional parameters when an additional iron line due to fluorescence was necessary to fit the data (the line energy was fixed at 6.4 keV).

3.2 Results

We show in Table 2 the hydrogen column of the warm absorber, Z, ϵ_0, $\dot{m}$, r_c and two mass estimates: one where we assumed no reflection and one where reflection was assumed. The other free parameters (N_e and the distance between the source and the absorber) did not have a significant effect on the resulting fit. In the reflection case, we calculated the viewing angle of the accretion region when this was possible, using estimates of the inclination and dipole offset in Cropper (1990). When this angle was not known, we assumed a viewing angle of $0°$ (giving maximum reflection): thus the best-fitting mass estimate lies somewhere between these two values.

In practise, the difference between the mass determinations with and without the reflection component is small. We find significantly better fits with a lower metallicity relative to solar for all the systems except QQ Vul (in the latter it was not possible to constrain Z). We would expect this result if we assume that most CVs are old objects.

The uncertainties for the two different mass estimates are also shown in Table 2. These were determined by stepping through a

range of white dwarf masses and fitting the spectrum as before while all the other free parameters were allowed to vary. The confidence range was taken at the 90 per cent level ($\Delta\chi^2=2.71$) for this single parameter. We did not determine the errors on other parameters such as $\dot{m}$, since this required large amounts of computer time.

We now discuss briefly the individual systems used in this study.

3.3 AM Her systems

AM Her. The data were divided into 10 spin phases, with the brightest sections (spin phase 0.4–0.8) being used in the fits. We fitted these four spin phase sections simultaneously keeping all the fitting parameters fixed except for the hydrogen absorption column of the warm absorber and iron line parameters which were allowed to vary in spin phase. The fit to the data and the residuals are shown in Fig. 4. There are no features apparent in the residuals. The viewing angle was determined using $i = 30°$, $\beta = 60°$ and the main accretion pole was closest to our line of sight at spin phase $\phi=0.65$ on the ephemeris reported in Heise & Verbunt (1988).

EF Eri. Data taken immediately after the absorption dip, covering 0.13 in spin phase, were used in the fit. The viewing angle was determined using $i = 58°$, $\beta = 27°$ and the main accretion pole was assumed to be closest to our line of sight at the peak of the X-ray flux.

BY Cam. Ishida et al. (1991) have already discussed these data and showed that the data could be split into two distinct states: one in which the spin of the white dwarf (the pulse state) was clearly seen and the other when it was in a flaring state. We used data from the pulse state in the fits. As the viewing angle to the dominant accretion pole in this system is uncertain we used a viewing angle of $0°$ for the reflection component. We chose a best-fitting mass between the no-reflection and reflection best fits ($M_{wd} = 1.08\,M_\odot$).

V834 Cen. Because V834 Cen was relatively faint when observed using *Ginga* and observed for a short time (there were pointing problems for part of the observation) we used a mean spectrum in the fit.
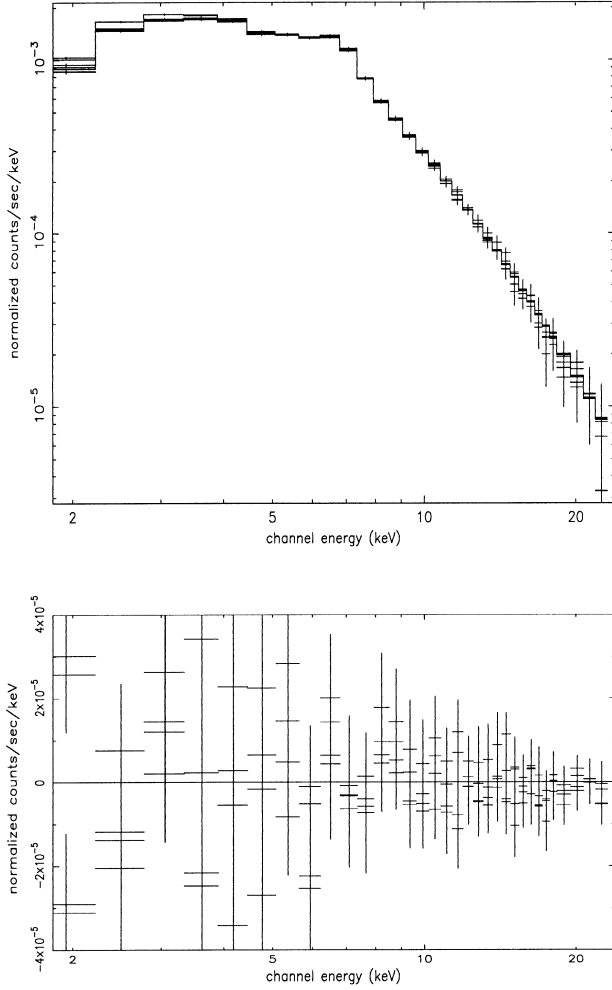
Figure 4. AM Her: the four sets of phase-resolved data along with their fits and residuals.

Figure 5. EX Hya: phase-resolved data along with the fit and residuals.

QQ Vul. Beardmore et al. (1995b) showed evidence for two accreting poles in QQ Vul using *ROSAT* and *Ginga* data. We therefore used data from only spin phase 0.1–0.55 when the hard X-rays were at maxima (see their Fig. 2) and likely to originate at one of the poles. As QQ Vul was relatively faint in hard X-rays, we fixed $Z = 1.0$ in the fits.

3.4 Intermediate polar systems

EX Hya. EX Hya shows a strong spin modulation in hard X-rays (Rosen et al. 1991). We used data covering 0.25 spin cycles centred on spin maximum. The fits to the data and the residuals are shown in Fig. 5.

AO Psc. A strong spin modulation is also seen in AO Psc. We thus extracted data covering 0.20 spin cycles centred on spin maximum.

FO Aqr. The hard X-ray light curve of FO Aqr is complex: unusually among IPs it shows a distinct orbital modulation in hard X-rays and the amplitude of the modulation of its spin folded light curve varies as a function of orbital phase. To constrain the mass of the white dwarf we extracted data from the brightest data spanning 0.15 spin cycles from orbital phases 0.05–0.30 and 0.40–0.65 and fitted their spectra simultaneously, keeping the same parameters free as in our analysis of the AM Her data. In the model including reflection the viewing angle was fixed at 0°. We took the best-fitting
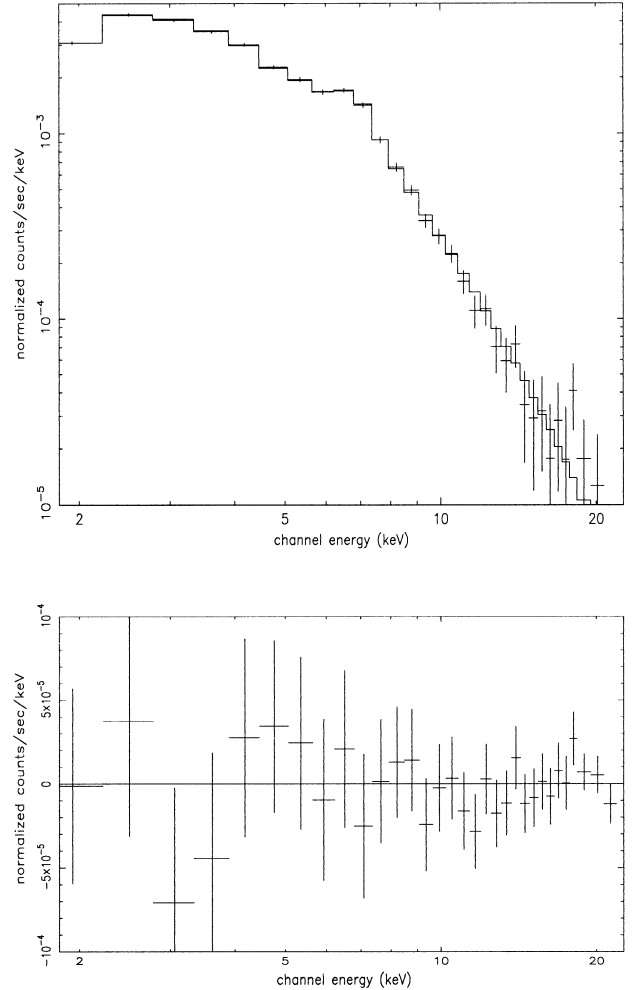
mass to be between the best-fitting mass derived from the models assuming reflection and no reflection ($M_{wd} = 1.22\,M_\odot$).

TV Col. As Ishida (1991) reported, the *Ginga* data showed no evidence for the light curve being modulated on the spin period, contrary to that seen in the *EXOSAT* data. However, Hellier, Garlick & Mason (1993) also showed that absorption dips were seen in the *EXOSAT* data spanning 0.3 of an orbital cycle. We extracted a spectrum from the *Ginga* data excluding orbital phases in which the absorption dips were present. We took the best-fitting mass to lie between the best-fitting mass derived from the models assuming reflection and no reflection ($M_{wd} = 1.20\,M_\odot$).

BG CMi. The X-ray data were modulated on the spin period of the white dwarf. Data were extracted from the bright phase of the spin cycle (excluding the central X-ray dip which is likely to be due to absorption). We took the best-fitting mass to lie between the best-fitting mass derived from the models assuming reflection and no reflection ($M_{wd} = 1.25\,M_\odot$).

TX Col. As in BG CMi, the X-ray data were modulated on the spin period. The fitted spectrum was extracted from the bright phase of the spin cycle (lasting 0.6 of a cycle). No evidence was found for a reflection component.

GK Per. GK Per was observed using MPC-2 mode in 1987 September. In this mode the spectral information is reduced in favour of timing information. Spectra were extracted from the full

cleaned data set and also from the bright phase of the spin cycle. The fits were not good ($\chi^2 > 3$), with the residuals greatest below 5 keV. The poor fits may be due to the presence of an accretion disc (in which case our model may not be applicable), or variable absorption over the orbital period (GK Per has a relatively long orbital period of 2 d, making it difficult to search for absorption dips during the orbital period). Thus no estimate of the mass of the white dwarf was possible.

PQ Gem. Because more than half of the *Ginga* data were contaminated with solar X-rays (Mason et al. 1992), a spectrum using all the cleaned data (but excluding 'day'time data) was used in the fitting. We took the best-fitting mass to lie between the best-fitting mass derived from the models assuming reflection and no reflection ($M_{wd} = 1.35\,M_\odot$).

AE Aqr. AE Aqr was faint in the *Ginga* observations (a mean of ~ 2 count s^{-1} and a maximum of ~ 6 count s^{-1}). To optimize the signal-to-noise ratio of the spectrum, we used data with an intensity above ~ 2 count s^{-1} in the spectral fit.

4 DISCUSSION

4.1 The model fits

The approach we have adopted in this investigation is to use physically appropriate models for our X-ray fits, incorporating a priori our observational and theoretical knowledge of the systems. While formally a 'lower order' fit, such as an absorbed single-temperature bremsstrahlung, may produce statistically satisfactory results in some cases, we contend that our procedure is justified in order to reduce systematic uncertainties in the derived parameters. This is particularly important in the mass derivations.

As noted in Section 3.2, the effect of the reflection component is relatively small. Moreover, the effect of the ionized absorber is also small above the 1.7-keV low-energy cut-off we used in our fits (the effect of this component could be mimicked by a partial covering absorber). Therefore by far the biggest component of our model contributing to the mass determination is the multi-temperature optically thin emission from the post-shock accretion flow. With this model we are able to achieve good fits to the data (Table 2).

4.2 Limitations of our assumptions

Although we have used the best models we have available for the fits, they contain several shortcomings, which we discuss below. With the advent of X-ray observatories with higher spectral resolution and throughput (such as *XMM*) it will be possible (and necessary) to improve on several of our restrictive assumptions.

One significant shortcoming is the geometry of our accretion structure. We assume that all of the emission from the accretion column is absorbed by the ionized absorber, irrespective of viewing angle, whereas in general there will be a viewing-angle dependence on the absorption, with some of the emission escaping the ionized absorber entirely. We also do not allow any local mass-transfer variation (leading to a height variation) in our column. Observations show that the accretion rate indeed varies across the accretion column for AM Her systems, and that these variations might be more important for IP systems. Moreover, we do not take into account any of the more structured models of the accretion region as noted in Section 2.

Regarding the stratified accretion column, our simple integration of the temperature strata and the MEKAL code itself assumes optically thin conditions. This assumption has been examined in the case of

EF Eri by Done et al. (1995), who calculated that the continuum emission is (mostly) optically thin while that of the the iron line is (mostly) optically thick, depending on the viewing angle. With data of higher resolution such as those from *ASCA*, such effects will need to be taken care of by treating the radiation transfer more appropriately. In the case of the lower resolution *Ginga* data which extend up to 20 keV, the mass determinations are dominated by the continuum and the errors introduced by our optically thin assumptions will be small.

The closed form analytic solution of Wu et al. (1994) assumes the classical strong shock conditions, and the thermal pressure upstream of the shock is zero. In addition, the flow is assumed to fall to zero at the surface of the white dwarf, and the temperature is assumed to be zero, rather than the photospheric temperature, or even that of a locally heated photosphere. This last assumption is probably the most problematic: Wu et al. (1994) note that it is unlikely to materially affect the bulk of the emission, but while this is probably true for the continuum, it is probably not true for the line emission, where the majority of emission is from the lower temperatures at the bottom of the column. Work is underway at relaxing these assumptions to improve the boundary conditions, but for the moment we retain them for the purposes of this investigation.

The optical depth considerations described above apply to the bulk of the accretion region, but in our stratified column the density reaches high values at the base of the column. In reality, the optical depth will exceed unity near the base of the column as the photosphere is approached. The radiative transfer in this lower region, and also in the ionized absorber, will need to be correctly treated.

The effects due to decoupling of electrons and protons have not been taken into account in calculating the structure of the emission region. When cyclotron cooling is efficient these effects (see e.g. Lamb & Masters 1979) may modify the emission spectra, thus leading to errors in the white dwarf mass estimates.

4.3 The white dwarf mass spectrum

The white dwarf masses of mCVs have been measured by several workers (Mukai & Charles 1987; Ishida 1991; Fujimoto & Ishida 1996; Hellier et al. 1996), and their results are tabulated in Table 3. We also include the white dwarf masses calibrated from the results given by Ishida (1991) from Wu et al. (1995) for comparison.

As can be seen, there are noticable discrepancies between the results listed in the table. The discrepancies are mainly due to different assumptions being used by different groups in deriving their mass estimates. For instance, Mukai & Charles (1987) used the radial velocity, together with an assumed orbital inclination, to deduce the white dwarf masses. For non-eclipsing systems, the inclination is not easy to constrain, but the mass estimate from this method is strongly dependent on the orbital inclination.

Ishida (1991) considered the X-ray continua of the systems and deduced the white dwarf mass from the X-ray spectral temperature. The X-ray spectra method is insensitive to the orbital inclination of the systems if only emission from the shock-heated region is considered. As Ishida (1991) considered the emission region to be homogeneous in temperature and density, the temperature he obtained is lower than the actual shock temperature, so that the resulting white dwarf masses are lower limits. A 'quick-fix' correction to the results of Ishida (1991) was made by Wu et al. (1995) who considered the temperature-weighting effects using structured models for the emission region obtained by hydrodynamic calculations. Their correction is generally applicable to both magnetic and non-magnetic systems, as bremsstrahlung and

Table 3. A comparison of the best-fitting estimates of the mass of the white dwarf in the systems discussed in this work. Data are taken from WCS: Wu et al. (1995); Ishida (1991); FI: Fuijmoto & Ishida (1996); MC: Mukai & Charles (1987); HMIF: Hellier et al. (1996); WHG: Welsh, Horne & Gomer (1994). The estimates of Ishida are lower limits.

Source	This work M_{wd}	WCS M_{wd}	Ishida M_{wd}	FI M_{wd}	MC M_{wd}	HMIF M_{wd}	WHG M_{wd}
AM Her	1.22	0.69	0.44		0.75		
EF Eri	0.88	0.57	0.39				
BY Cam	1.08	1.10	0.63				
V834 Cen	0.51	0.51	0.33				
QQ Vul	1.12	1.20	0.66		0.58		
EX Hya	0.52	0.35	0.24	0.48			
AO Psc	0.40	0.50	0.32			0.40	
FO Aqr	1.22	0.80	0.49				
TV Col	1.20	0.88	0.52				
BG CMi	1.25	0.85	0.50				
TX Col	0.55						
PQ Gem	1.35	0.65	0.31				
AE Aqr	0.3						0.89

Figure 6. The mass spectrum of field white dwarfs (Bergeron et al. 1992), white dwarfs in CVs (Webbink 1990) and from this study (Table 3).

cyclotron cooling are considered. The white dwarf masses after calibration are indeed higher than the original values. However, the 'quick-fix' method of Wu et al. (1995) omits the density-weighting effects, so that the white dwarf masses are still underestimated. In this work, the temperature and density structures of the emission region are considered explicitly in calculating the X-ray continuum, and other significant effects, such as reflection and absorption, are also included, thus the resulting white dwarf masses are expected to be more accurate than previous continuum spectral methods.

Recently, the white dwarf masses of two IPs, EX Hya and AO Psc, were determined by fitting the X-ray emission lines of the high-resolution *ASCA* data (Fujimoto & Ishida 1996; Hellier et al. 1996) with model line emission from a structured emission region (Aizu 1973). The white dwarf masses we have obtained for these two systems are in good agreement with the values deduced by line spectral methods.

Note that owing to an error in the software fits, in which the density weighting was not performed correctly, previously calculated masses in Cropper, Ramsay & Wu (1997) and Wu, Cropper & Ramsay (1997) are incorrect. Nevertheless the masses given in these papers are similar to calibrated masses given in Wu et al. (1995) as the weighting of the emission due to density structure is omitted in both.

As a first glance, the masses we derive seem to be higher than expected, with means for the AM Her systems of $0.96\,M_\odot$ and that for the IPs of $0.93\,M_\odot$ (excluding the mass of AE Aqr which has a large error). We have made checks with multi-temperature bremsstrahlung (rather than MEKAL) fits, and these yield similar and slightly higher (by $\sim 0.03\,M_\odot$) masses. We have carried out other tests including varying the parameters such as abundance, or those governing the warm absorber, and have found that there is only minimal effect on the derived masses. We have also performed consistency checks on the luminosity and emitting volume for different mass-transfer rates. We have considered the appropriateness of our assumptions: as noted earlier, optical depth effects and inadequate boundary conditions at the base of the column affect low-energy photons most significantly so we have performed fits assuming increasing low-energy cut-offs (2 keV then 3 keV and
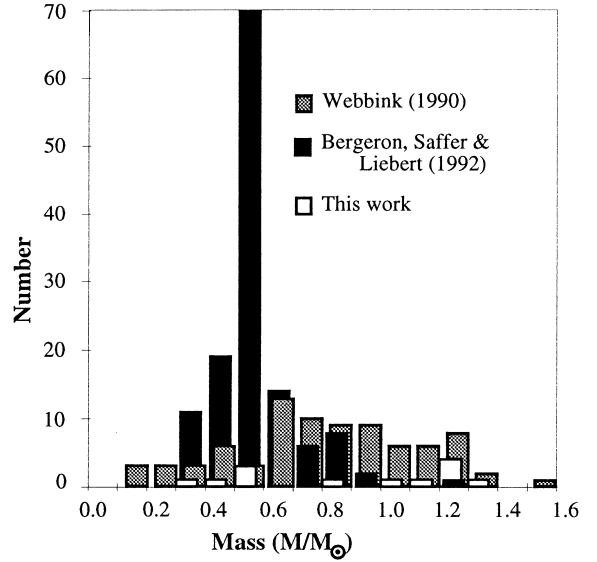
5 keV) but find no systematic change (other than increasing uncertainties on the fit) in the derived masses. Thus we conclude the derived masses are robust.

The mass spectrum of white dwarfs has been a subject of attention, for both white dwarfs in binaries and isolated white dwarfs. There are two commonly quoted mass distributions: the compilation of masses of white dwarfs in CV systems by Webbink (1990), and the compilation of masses of isolated white dwarfs by Bergeron, Saffer & Liebert (1992). Webbink (1990) listed the white dwarf masses of 84 CV systems. However, the sources of the data were not stated in detail, and we are unable to assess the uncertainties, although there are quality flags associated with the data in the size of the markers in fig. 2 of Webbink (1990). The Bergeron et al. (1992) compilation consists of 129 DA white dwarfs. The white dwarf masses were determined by fitting hydrogen line profiles. [The mass spectrum was rededuced by Liebert & Bergeron (1995) with stars from the PG sample, including stars with $T_{eff} \geq 40\,000\,K$, but the inclusion of these masses results in only minor changes to the peak of the mass distribution.]

In Fig. 6, we show the mass spectrum derived in this work, together with the mass spectra of Webbink (1990) (with both magnetic and non-magnetic systems aggregated) and of Bergeron et al. (1992). The isolated white dwarf distribution is peaked at $\sim 0.6\,M_\odot$, whereas the distribution of the mass of white dwarfs in CV systems is extended to higher masses. Our mass compilation is too small to draw any firm conclusions. We note, however, that the mean mass of the sample is higher than that of Webbink (1990). This is true even if only the magnetic CVs in that sample are selected (mean mass $\sim 0.85\,M_\odot$ as opposed to $\sim 0.94\,M_\odot$ of our sample).

Since first pointed out by Warner (1973), the significance of the apparently more massive white dwarfs occurring in binary systems than as isolated white dwarfs has been widely debated. Whether or not the instrinsic mass spectra of the two groups of white dwarfs are different has not been resolved by this investigation. Moreover, it is undisputable that strong selection effects are present (Ritter & Burkert 1986).

White dwarf mass spectra of close binaries were calculated from theoretical considerations by Politano (1990) and de Kool (1992). Their calculations predict a minimum in the mass spectrum at $\sim 0.5\,M_\odot$ between the two humps, corresponding to the two populations (He and C–O) of white dwarfs. This result seems to be consistent with the distribution given in Webbink (1990), and also our sample, to the extent that the small sample size permits. However, there are many subtle assumptions in any population synthesis for binary stars. The physics of one of the crucial processes in the synthesis calculations – the treatment of the common envelope phase – is still not well understood. Moreover, while the mass of isolated white dwarfs is determined by the progenitor stars, the mass of a white dwarf in a binary system depends also on the subsequent interaction with its companion star. Furthermore, the situation can be complicated by nova explosions, which can cause white dwarfs in CV systems to lose substantial mass. The present knowledge of mass stripping by nova explosions, of the mass-transfer process and of CV orbital evolution is inadequate to permit a precise prediction of the mass spectrum for white dwarfs in binary systems. Thus, any conclusions regarding the apparently observed differences in the mass spectra of white dwarfs in single and binary systems should be treated with circumspection.

5   CONCLUSIONS

We have generated a model for the X-ray emission from magnetic CVs based on our present understanding of the structure of these systems. This includes a multi-temperature optically thin emission component, together with reflection from the white dwarf surface and an ionized absorber. We find that the model provides good fits to the observed spectra of 13 systems in the archive *Ginga* data.

The derived masses are higher than given in Wu et al. (1995) and Ishida (1991). Our method takes care of the essential effects such as temperature and density weighting of the emission, reflection from the white dwarf surface and absorption by pre-shocked matters.

The derived white dwarf masses will be of value in further investigations of each system, but we have not explored the implications of our results for past findings in this paper.

We have compared the mass distribution we calculated to that for the isolated white dwarfs and also to the spectrum of white dwarf masses in CVs. As far as our small sample size permits, we find that our mass distribution is consistent with that for CVs in general (although with a slightly higher mean mass) and with the predicted mass spectrum from CV evolutionary models.

This investigation has illuminated several aspects that could be pursued in future work. One important but difficult improvement would be the updating of the model to include more recent views of the accretion region (as noted in Section 2) with, for example, the inclusion of blobby accretion. This could be used to attempt to distinguish the various accretion scenarios, or, for example, to investigate the soft X-ray spectral changes during flare events in AM Her (Ramsay, Cropper & Mason 1996). Other improvements would be: to treat the boundary conditions in our accretion structure more satisfactorily, both in the pre-shock flow and near the white dwarf surface; to improve the radiative transfer both in the lines from the post-shock flow and in the absorbing material in the system; and to improve the reflection component by including self-consistently the fluorescent lines and the radial dependence of the temperature structure in the white dwarf.

REFERENCES

Aizu K., 1973, Prog. Theoret. Phys., 49, 1184
Aldrovani S. M. V., Péquignot D., 1973, A&A, 25, 137
Andronov I. L., 1987, Astron. Nachr., 308, 229
Arnaud K. A., 1996, in Jacoby G., Barnes, J., eds, ASP Conf. Ser. 101, Astronomical Data Analysis Software and Systems V. Astron. Soc. Pac., San Francisco, p. 17
Bailey J. A., 1995, in Buckley D. A. H., Warner B., eds, ASP Conf. Ser. 85, Cape Workshop on Magnetic Cataclysmic Variables. Astron. Soc. Pac., San Francisco, p. 10
Beardmore A. P., Done C., Osborne J. P., Ishida M., 1995a, MNRAS, 272, 749
Beardmore A. P., Ramsay G., Osborne J. P., Mason K. O., Nousek J. A., Baluta C., 1995b, MNRAS, 273, 742
Bergeron P., Saffer R. A., Liebert J., 1992, ApJ, 394, 228
Beuermann K., 1988, in Coyne G. V., Magalhaes A. M., Moffat A. F. G., Schulte-Ladbeck R. E., Tapia S., Wickramasinghe D. T., eds, Polarized Radiation of Circumstellar Origin. Vatican Obs. Publ., p. 125
Beuermann K., Burwitz V., 1995, in Buckley D. A. H., Warner B., eds, ASP Conf. Ser. 85, Cape Workshop on Magnetic Cataclysmic Variables. Astron. Soc. Pac., San Francisco, p. 99
Beuermann K., Stella L., Patterson J., 1987, ApJ, 316, 360
Brickhouse N. et al., 1995, Legacy (Journal of HEASARC), 6, 4
Buff J., McCray R., 1974, ApJ, 189, 147
Cropper M., 1987, Ap&SS, 131, 651
Cropper M., 1990, Space Sci. Rev., 54, 195
Cropper M., Ramsay G., Wu K., 1997, in Wickramasinghe D. T., Bicknell G. V., Ferrario L., eds, ASP Conf. Ser. 121, Proc. IAU Colloq. 163, Accretion Phenomena and Related Outflows. Astron. Soc. Pac., San Francisco, p. 413
de Kool M., 1992, A&A, 261, 188
Done C., Mulchaey J. S., Mushotzky R. F., Arnaud K. A., 1992, ApJ, 395, 275
Done C., Osborne J. P., Beardmore A. P., 1995, MNRAS, 276, 483
Frank J., King A. R., Lasota J. P., 1988, A&A, 193, 113
Fujimoto R., Ishida M., 1996, ApJ, 474, 774
Hakala P. J., 1995, A&A, 296, 164
Hamada T., Salpeter E. E., 1961, ApJ, 134, 683
Hatchett S., Buff J., McCray R., 1976, ApJ, 206, 847
Heise J., Verbunt F., 1988, A&A, 189, 112
Hellier C., Garlick M. A., Mason K. O., 1993, MNRAS, 260, 299
Hellier C., Mukai K., Ishida M., Fujimoto R., 1996, MNRAS, 280, 877
Imamura J. N., Durisen R. H., Lamb D. Q., West G. J., 1987, ApJ, 313, 298
Ishida M., 1991, PhD Thesis, Univ. of Tokyo
Ishida M., Silber A., Bradt H. V., Remillard R. A., Makishima K., Ohashi T., 1991, ApJ, 367, 270
Ishida M., Sakao T., Makishima K., Ohashi T., Watson M. G., Norton A. J., Kawada M., 1992, MNRAS, 254, 647
King A. R., Lasota J.-P., 1979, MNRAS, 188, 653
Kolb U., 1993, A&A, 279, L5
Kuijpers J., Pringle J. E., 1982, A&A, 114, L4
Kylafis N. D., Lamb D. Q., 1982, ApJS, 48, 239
Lamb D. Q., Masters A. R., 1979, ApJ, 234, L117
Langer S. H., Chanmugam G., Shaviv G., 1982, ApJ, 258, 289

Liebert J., Bergeron P., 1995, in Koester D., Werner K., eds, White Dwarfs. Springer Verlag, Berlin, p. 12

Lightman A. P., White T. R., 1988, ApJ, 335, 57

Mason K. O. et al., 1992, MNRAS, 258, 749

Masters A. R., 1978, PhD Thesis, Univ. of Illinois (Urbana-Champaign)

Mewe R., Gronenschild E. H. B. M., van den Oord G. H. J., 1985, A&AS, 62, 197

Mewe R., Kaastra D. S., Liedahl D. A., 1995, Legacy (Journal of HEASARC), 6, 16

Morrison R., McCammon D., 1983, ApJ, 270, 119

Mukai K., Charles P., 1987, MNRAS, 226, 209

Nauenberg M., 1972, ApJ, 175, 417

Norton A. J., Watson M. G., King A. R., Lehto H. J., McHardy I. M., 1992a, MNRAS, 254, 705

Norton A. J., McHardy I. M., Lehto H. J., Watson M. G., 1992b, MNRAS, 258, 697

Patterson J. O., 1994, PASP, 106, 209

Politano M. J., 1990, in Mauche C. W., ed., Accretion Powered Compact Binaries. Cambridge Univ. Press, Cambridge, p. 421

Ramsay G., Mason K. O., Cropper M. S., Watson M. G., Clayton K. L., 1994, MNRAS, 270, 692

Ramsay G., Cropper M., Mason K. O., 1995, MNRAS, 276, 1382

Ramsay G., Cropper M., Mason K. O., 1996, MNRAS, 278, 285

Ritter H., Burkert A., 1986, A&A, 158, 161

Rosen S. R., Mason K. O., Córdova F. A., 1988, MNRAS, 231, 549

Rosen S. R., Mason K. O., Mukai K., Williams O. R., 1991, MNRAS, 249, 417

Rothschild R. E. et al., 1981, ApJ, 250, 723

Stockman H. S., 1988, in Coyne G. V., Magalhaes A. M., Moffat A. F. G., Schulte-Ladbeck R. E., Tapia S., Wickramasinghe D. T., eds, Polarized Radiation of Circumstellar Origin. Vatican Obs. Publ., p. 237

Turner M. J. L. et al., 1989, PASJ, 41, 345

van Teeseling A., Kaastra J. S., Heise J., 1996, A&A, 312, 186

Warner B., 1973, MNRAS, 162, 189

Warner B., 1995, Cataclysmic Variable Stars. Cambridge Univ. Press, Cambridge

Webbink R. F., 1990, in Mauche C. W., ed., Accretion Powered Compact Binaries. Cambridge Univ. Press, Cambridge, p. 177

Welsh W. F., Horne K., Gomer R., 1994, MNRAS, 257, 649

Wickramasinghe D. T., 1988, in Coyne G. V., Magalhaes A. M., Moffat A. F. G., Schulte-Ladbeck R. E., Tapia S., Wickramasinghe D. T., eds, Polarized Radiation of Circumstellar Origin. Vatican Obs. Publ., p. 1

Wickramasinghe D. T., Wu K., 1994, MNRAS, 266, L1

Woelk U., Beuermann K., 1996, A&A, 306, 232

Wu K., 1994, Proc. Astron. Soc. Aust., 11, 61

Wu K., Chanmugam G., Shaviv G., 1994, ApJ, 426, 664

Wu K., Chanmugam G., Shaviv G., 1995, ApJ, 455, 260

Wu K., Cropper M., Ramsay G., 1997, in Bedding T. R., Booth A. J., Davis J., eds, Proc. IAU Symp. 189, Fundamental Stellar Properties: the interaction between observations and theory. Kluwer, Dordrecht, p. 115

Zdziarski A. A., Magdziarz P., 1996, MNRAS, 279, 21